Estimation of Shear Strength Characteristics of Unreinforced and Reinforced Barind Soil Using Stress Path Method

S. A. MOFIZ[1]

[1]Department of Civil Engineering, Rajshahi University of Engineering & Technology, Bangladesh (samofiz@gmail.com)

Abstract

The study assesses the possible effects of stress path on reinforced and unreinforced Barind soil simulating the different loading path similar to what is expected in the field. The testing program concentrated on a series of consolidated-drained triaxial compression and extension tests of expansive soil specimens on 50 mm diameter and 100 mm high samples. Testing was carried out at consolidating pressures ranging between 0.10-0.60 MPa using Geotechnical Digital System computer control triaxial apparatus. Test results show that reinforced soils exhibit higher failure strains and volume contraction than unreinforced soils. Reinforced soils with non-woven geotextile exhibit higher failure strains, strength and coefficient of interface friction than unreinforced Barind soil. It is also observed that the percentage increase in the strength is stress path dependent. But the shear parameters of the expansive soils are independent of the various stress paths followed.

Keywords: *Barind Soil, Unreinforced and Reinforced Soil, Shear Strength, Triaxial Test, Stress Path.*

1 Introduction

The stress strain characteristics in the soils due to a given increment of stress vary considerably depending on the stress-level and confining pressure. In the field, soil elements undergo different stress paths depending upon the loading condition. Reinforced soil has gained popularity due to its extensive application in various problems such as embankments, retaining walls, pavements, foundations, etc. These problems are often analysed by finite element method. The non-linear stress-strain relationship, which may be highly dependent on the confining stress, was formulated and implemented for finite element analysis by Ling and Tatsuoka (1992). Ling and Tatsuoka (1994) conducted a study on silty clay reinforced with three types of geosynthetics, two geotextiles, and a geogrid under plane strain conditions. Taha et al. (1999) demonstrated the behaviour of georeinforced residual soil using drained triaxial samples, showed that the reinforced systems increased strength-deformation properties in a significant manner. Ashmawy et al. (1999) reported that reinforced soils exhibit an improvement in strength-deformation characteristics under monotonic loading conditions, due to the additional "pseudo" confinement caused by the lateral restraint and shear mobilization. The present research works is aimed to determine the stress-strain mechanism between the reinforcement and barind soil using stress path tests. However, with respect to barind soil, both its interaction mechanism and its failure behaviour in soil composites are not well understood due to limited study. Thus, a thorough investigation of the soil reinforcement interaction was conducted. The simplified prediction procedures to determine the strength of reinforced and unreinforced soils for various stress paths are presented. An attempt was undertaken to determine the coefficient of interface friction from test results. Prediction charts are presented for different friction angle of soil and number of reinforcement layers.

2 Properties of Barind Soil and Geosynthetics

Barind soils often found in tropical or semi-tropical area are formed from intense weathering of rocks under consistently high temperature and rainfall. In this work, the disturbed soil was collected from the northern part of Bangladesh. The soil is reddish in colour and classified as CH in the Unified Classification System (USCS). The soil contains about 50 % clay, 35 % silt, 15 % sand and no gravels. The maximum dry density from the standard Proctor test was 15.65 kN/m^3 and the optimum moisture content was about 25.5%. In this research work, a non-woven geotextile was used as the reinforcement material. This group of geotextiles consists of mechanically bonded (needle punched) continuous filaments made from UV-stabilized polypropylene. The tensile strength properties of the reinforcement were determined following (ASTM 2013). The maximum tensile strength from the tests was obtained 17.68 kN/m and 19.12 kN/m in the longitudinal and transverse direction, and the corresponding elongations were about 70%, 52% respectively.

3 Test Procedure

In this study, twelve consolidated drained triaxial stress path tests were performed on the unreinforced barind soil as shown in Figure 1. The six stress path tests were followed using 50mm diameter and 100mm high cylindrical triaxial specimen for both unreinforced and reinforced soil. Based on the unit weight and the volume of the triaxial mold, the total weight of the soil was divided into three equal portions and compacted inside the mold in layers of equal height. For reinforced specimen, two circular discs of non-woven geotextile were placed at the 1/3 height from the top and 1/3 height from the bottom of the specimens. A rate of 0.15 mm/min for compression on a triaxial press was adopted, and each layer was compacted following the approach by Cui and Delage (1996) to ensure Proctor maximum density with a double piston system. The tests reported in this paper for both unreinforced and reinforced soil were carried out under consolidation pressure in the range 100-600 kPa. A strain rate of 0.0015 %/min was used to ensure no pore pressure change as required in a drained test. The computer controlled triaxial (GDS) system was adapted to carry out all the stress path tests. A microprocessor collects the data from transducers automatically at prescribed intervals. The data were transmitted by the controlling microprocessor for recording, processing and production of results, which could be displayed on the screen

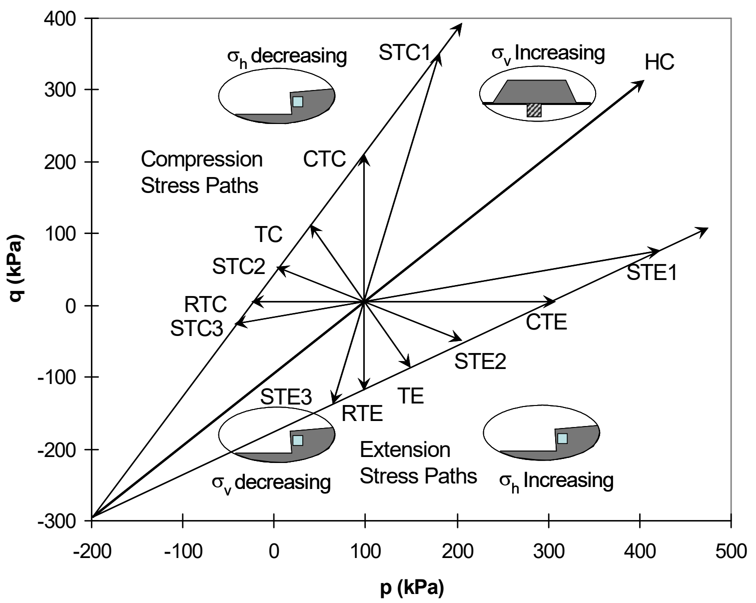

Figure 1. Schematic diagram of the different triaxial stress paths

4 Test Result and Discussions

For compression and extension stress path test, the stress-strain and volume change plots for the different stress paths at a consolidation pressure σ_c = 100 kPa are presented in Figure 2(a) and 2(b). In the compression stress path, failure strains (ε_a) are maximum for STC1 stress path and minimum for STC3. At low stress levels the volume change characteristics exhibits volume contraction for STC1 and CTC stress path whereas expansions for STC2 and STC3 stress path. As one moves from STC1 path to STC3 path, the volume change contraction decreases and the soil starts expansion even at low stress levels. This phenomenon is most likely due to decreasing confining pressure and dependent on the stress path followed. In the extension side, the negative failure strain ($-\varepsilon_a$) is maximum in STE1 stress path and minimum for STE3 stress paths. Test observations of STE1 and CTE paths indicate that the volume contraction is higher due to the gradual increase of cell pressure. The volume contraction decreases from STE2 to TE whereas expansion behaviour was observed for RTE and STE3 paths. This contraction-expansion behaviour is the result of the gradual decrease of axial stress and incremental increase of confining pressure.

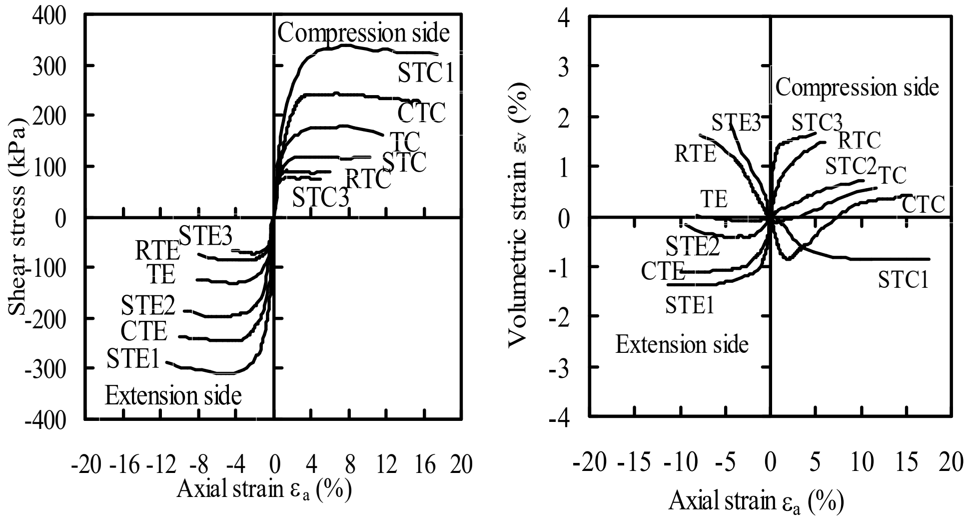

Figure 2. Behaviour of soil at consolidation pressure (σ_c=100 kPa) for different stress paths: (a) shear stress vs. axial strain (b) volumetric strain vs. axial strain.

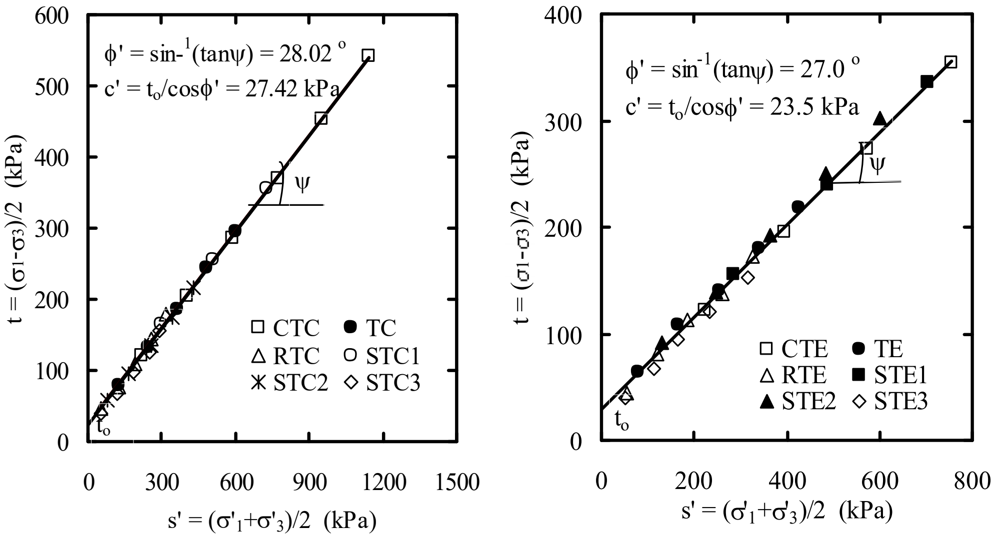

Figure 3. MIT failure envelopes for unreiforced barind soil: (a) compression stress paths (b) extension stress paths.

In this research, it is observed that the cohesion intercept and the angle of internal friction of the barind soil for the compression stress path are higher than that for the extension stress path. This is possibly the mobilised shear strength is higher due to the soil particles try to reconsolidate under compression loading. For the extension path, it has slightly lower values because the shear load is applied in the lateral or reverse direction which may cause soil to fail under tensile forces. The failure envelopes of unreinforced soil in terms of $s' = (\sigma'_1+\sigma'_3)/2$, $t = (\sigma_1-\sigma_3)/2$ for the compression and extension stress paths are presented in Figure 3(a) and Figure 3(b). Test results show that the shear strength parameters are slightly different in compression and extension loadings. The cohesion and angle of internal friction of unreinforced soil under compression and extension loading are c' = 27.42 kPa, ϕ' = 28.02^o and c' = 23.50 kPa, ϕ' = 27.00^o respectively. However, in each side, the parameters are independent of the stress path. The mode of failure of the single layered soil samples is observed by two bulging failures. For two layered reinforced soil, it is observed that the failure occurs in the soil composites by three small bulges over the length of the samples. As expected, the non-woven geotextiles reinforced samples exhibit higher shear strength than unreinforced samples and the maximum shear strength were attained at higher axial strains. This increase of shear strength is caused by an increase of the confining pressure in the soil between the reinforcement layers which depends on the interface friction resistance along the reinforcement. The shear strength parameters for a two layered non-woven geotextile reinforced soils are determined from the MIT stress path method. The cohesion intercept and angle of internal friction for a two layered reinforced soil under compression and extension loading are c'=43.85 kPa, ϕ'=32.4^{o} and c' = 38.56 kPa, ϕ' = 30.81^{o} as shown in Figure 4. It is also observed that the reinforced soils exhibit higher failure strain and shows about 20% to 43% higher than that of unreinforced soils. Comparison of strength parameters and failure strains for unreinforced and reinforced soil are presented in Table 1 and Table 2.

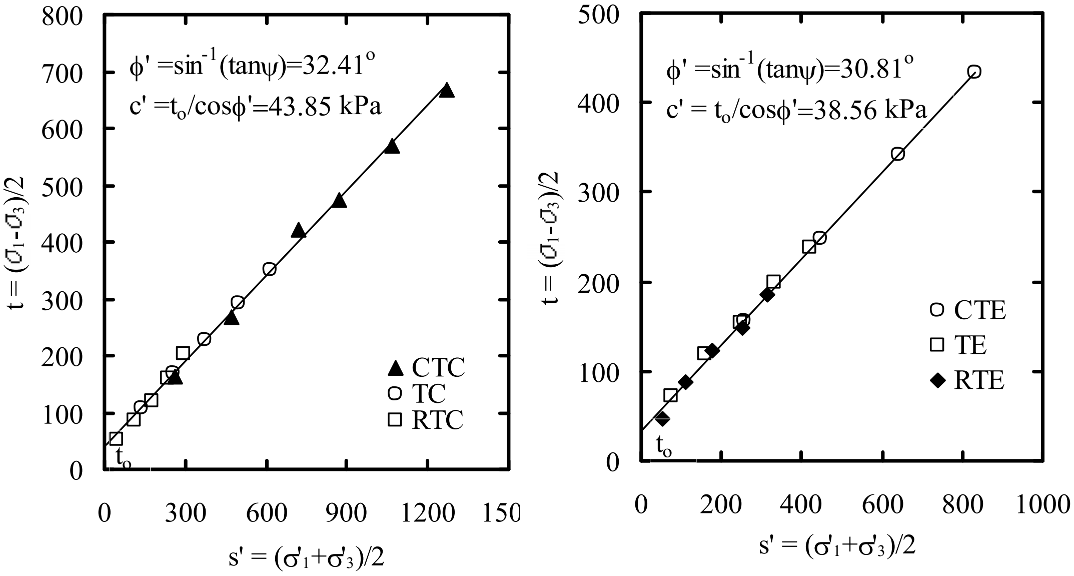

Figure 4. MIT failure envelopes for a two layered non-woven geotextile reinforced soil: (a) compression stress path (b) extension stress path

Table 1. Comparison of strength parameters for unreinforced and reinforced soil

Types of specimen	Stress path	Cohesion, c′ (kPa)	Friction angle, ϕ'^{o}	Increase of parameters over unreinforced soil	
				c′	ϕ'^{o}
Unreinforced	Compression	27.42	28.02	-	-
	Extension	23.50	27.00	-	-
Reinforced	Compression	43.85	32.41	16.43	4.39
	Extension	38.56	30.81	15.06	3.81

Table 2. Comparison of failure strains of unreinforced and reinforced soil at consolidation pressure σ_c = 100 kPa

Stress paths	Failure strain of unreinforced soil (%)	Failure strains of reinforced soil (%)	Increase of failure strains over unreinforced soil (%)
CTC	7.91	11.33	43.23
TC	7.15	9.69	35.52
RTC	3.84	5.18	34.89
CTE	5.96	8.22	37.92
TE	4.95	6.87	38.78
RTE	3.82	5.08	32.98

5. Conclusions

A brief research summary of the experimental study and the stress-strain characteristics of unreinforced and reinforced Barind soil are given. The stress-strain and volume change behaviour for Barind soil are highly stress paths dependent. Maximum percentage of increase in the strength exhibits for CTC path and minimum for RTC path. For extension paths, the percentage increase is maximum for CTE path and minimum for RTE path. The shear strength parameters for geotextile reinforced soils are determined from the MIT stress path method. It is also observed that the percentage increase in the strength is stress path dependent. But the shear strength parameters of the Barind soil are independent of the various stress paths followed. As expected, the reinforced samples exhibit higher shear strength than unreinforced samples and the maximum shear strength were attained at higher axial strains. This increase of shear strength is caused by an increase of the confining pressure in the soil between the reinforcement layers which depends on the interface friction resistance along the reinforcement.

References

Ashmawy, A.K., Bourdeau, P.L., Drnevich, V.P. & Dysli, M. (1999). Cyclic response of geotextile- reinforced soil. Soils and Foundations, 39(1): 43-52.

ASTM (2013). Testing of geotextiles and related products. Annual Book of ASTM standards, 04.08. D4595.

Cui, Y.J. & Delage, P. (1996). Yielding and plastic behaviour of an unsaturated compacted silt. *Geotechnique*, 46(2): 291-311.

Ling, H.I. & Tatsuoka, F. (1992). Nonlinear analysis of reinforced soil structures by modified CANDE (M-CANDE) Geosynthetic-Reinforced Soil Retaining Walls, Jonathan Wu, (ed), 279-296. Rotterdam: Balkema.

Ling, H.I. & Tatsuoka, F. (1994). Performance of anisotropic geosynthetic-reinforced cohesive soil mass. Journal of Geotechnical Engineering, ASCE, 120(7): 1167-1184.

Taha, M.R, Mofiz, S.A. & Hossain, M.K. (1999). Behaviour of georeinforced residual soil in triaxial test. Proc. World Engineering Congress 99-Towards Engineering Vision: *Global Challenges and Issues*, 19th –22nd July, 1999, Kuala Lumpur, 175-180.